Development of a 6-DOF Model for Underwater Bomb Trajectory Prediction with Application to the Stand-off Assault Breaching Weapon Fuse Improvement (SOABWFI)

Peter C. Chu

Naval Ocean Analysis and Prediction Laboratory
Naval Postgraduate School, Monterey CA 93943, USA

Abstract

To support the development and evaluation of the Stand-off Assault Breaching Weapon Fuse Improvement (SOABWFI) program, a 6-DOF computational bomb maneuvering model is developed to accurately predict the trajectory pattern, velocity and orientation of the warheads when they are released from any of the various dispense concepts. Tests such as $1/12^{th}$ scaled MK-84 bomb experiments with various water-entry velocities at SRI (near 1000 ft/s) and NPS (near 400 ft/s) provide good data on bomb trajectory and some insight into bomb orientation. With these data, semi-empirical formulas are derived for calculating drag/lift coefficients with fast water-entry, and used by the 6-DOF bomb trajectory model. This model development provides a tool to determine accurately underwater (full-size) bomb trajectory path so that the final detonation position relative to target position can be predicted.

1   Introduction

One of the greatest threats to U.S. sea-based power projection in littoral areas are mines, which inhibit or prevent amphibious landings of troops and military equipment. Guided general-purpose bombs represent an existing, rapidly deployable, building block for developing an effective system for use against mines. The Joint Direct Attack Munition (JDAM) Assault Breaching System (JABS) have proven effective to clear proud mines on beach and surf zones but not on VSW-zone (Fig. 1). More recent initiatives have concentrated on extension of the JABS from beach/surf zones to VSW-zone, i.e., the Stand-off Assault Breaching Weapon Fuse Improvement (SOABWFI) program.

Fig. 1. Successful mine breaching in beaches/surf zones by JABS (from Almquist 2006).

Bomb released from the aircraft leads to a high water-entry speed (up to 1000 ft/s) where a cavity is developed around the body. Generally the bomb has a nose and a tail. Depending on the tail design, the bomb can be stabilized in the cavity as the tail hits the cavity wall. Some times the tail is torn off and the body is unstable. Penetration into the seabed by bombs with a tangent Ogive nosecone is not well predicted. The bomb will deviate from its original path. Development of bomb maneuvering prediction model is an urgent need for mine removal in VSW-zone. Recently, this program will be extended from shallow water to deep water to permit rapid, effective, transition from sea to land.

The primary objective of this overall effort is the development of a six degrees of freedom (6-DOF) model to predict underwater high-speed bomb trajectory and orientation. This model will be used in SOABWFI to provide accurate predictions of underwater bomb location, velocity and, orientation from launch until final detonation.

In this study, an inverse model is developed for determining the drag/lift coefficients from the rigid-body's trajectory and orientation. Then a bomb strike experiment is conducted to collect the data for the trajectory and orientation. Using the experimental data, semi-empirical formulas are derived for the drag/lift coefficients.

2 Hydrodynamic Force and Torque

Consider an axially symmetric rigid-body with length L such as bomb falling through water column with the centers of mass (c_m) and volume (c_v) on the main axis (Fig. 2). The position of the body is represented by the position of c_m,

$$\mathbf{r}(t) = x\mathbf{i} + y\mathbf{j} + z\mathbf{k}, \tag{1a}$$

which is called the translation. The positions of the two end-points (such as head and tail points) are represented by $\mathbf{r}_h(t)$ and $\mathbf{r}_t(t)$. The difference between the two vectors in nondimensional form

$$\mathbf{e} = \frac{\mathbf{r}_h - \mathbf{r}_t}{\left|\mathbf{r}_h - \mathbf{r}_t\right|}, \tag{1b}$$

is the unit vector representing the body's main axis direction. The translation velocity is given by

$$\frac{d\mathbf{r}}{dt} = \mathbf{u}, \qquad \mathbf{u} = V\mathbf{e}_v. \tag{2a}$$

where V and $\mathbf{e}_v$ are the speed and unit vector of the rigid-body velocity.

Let $\mathbf{v}$ be the water-to-body relative velocity (called the relative velocity). If the water velocity is much smaller than the rigid-body velocity, the water-to-body relative velocity can be approximately given by

$$\mathbf{v} \approx -\mathbf{u} = -V\mathbf{e}_v . \tag{2b}$$

Usually the two vectors ($\mathbf{e}$, $\mathbf{e}_v$) are not parallel and their vector product leads to a unit attack vector

$$\mathbf{e}_\alpha = \frac{\mathbf{e}_v \times \mathbf{e}}{\sin \alpha}, \tag{3}$$

where α is the angle between ($\mathbf{e}$, $\mathbf{e}_v$). For a two dimensional motion, if (β, γ) are the elevation angles of the rigid body and its velocity, the difference $\alpha = \beta - \gamma$, is the water attack angle (Fig. 2).

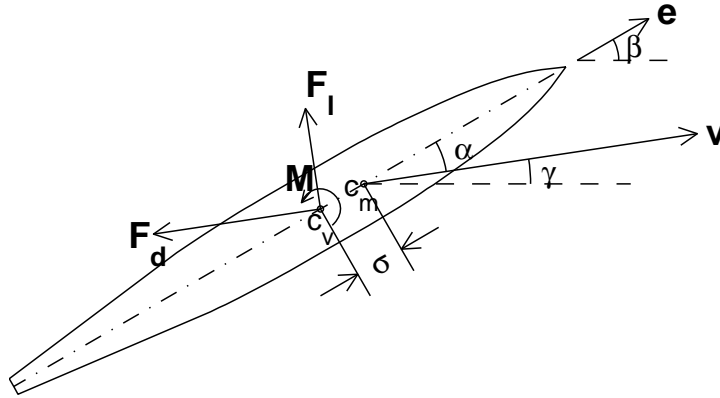**Fig. 2. Shift of the exerted point of the drag/lift forces from COF to COV with an extra torque M_t. Here, (α, β, γ) are the attack angle, elevation angels of the body and its velocity.**

Hydrodynamic force on a rigid body consists of a drag force ($\mathbf{F}_d$)

$$\mathbf{F}_d = f_d \mathbf{e}_d , \quad \mathbf{e}_d = -\mathbf{e}_v , \tag{4}$$

and a lift force ($\mathbf{F}_l$)

$$\mathbf{F}_l = f_l \mathbf{e}_l , \quad \mathbf{e}_l = \frac{(\mathbf{e}_v \times \mathbf{e}) \times \mathbf{e}_v}{|(\mathbf{e}_v \times \mathbf{e}) \times \mathbf{e}_v|} . \tag{5}$$

Their magnitudes are determined by the drag and lift laws,

$$f_d = \frac{1}{2} C_d \rho A_w V^2, \quad f_l = \frac{1}{2} C_l \rho A_w V , \tag{6}$$

where ρ is the water density; A_w is the under-water area of projection; and (C_d, C_l) are the drag and lift coefficients. Let $\boldsymbol{\sigma}$ be the vector from the center of mass (COM) to the center of volume (COV), or $\boldsymbol{\sigma} = \sigma\mathbf{e}$. The center of the hydrodynamic force (COF) is the location where the fulcrum is chosen with zero torque. In fact, the hydrodynamic torque is calculated from the resultant drag and lift force exerted on COF with COM as the fulcrum ($\mathbf{M}_h^*$). If we shift the exerted point of the resultant drag and lift force from COF to COV, the torque ($\mathbf{M}_h^*$) contains two parts

$$\mathbf{M}_h^* = \mathbf{M}_h + \mathbf{M}_t, \quad \mathbf{M}_h = \sigma\mathbf{e}\times(\mathbf{F}_d + \mathbf{F}_l), \quad \mathbf{M}_t = M_t\mathbf{e}_\alpha, \tag{7}$$

where $\mathbf{M}_h$ is the hydrodynamic torque with the resultant drag and lift force exerted on COV, and $\mathbf{M}_t$ is the torque caused by the shift of the exerting point from COF to COV. Here, the magnitude of $\mathbf{M}_t$ is calculated by the drag law

$$M_t = \frac{1}{2}C_m\rho A_w L_w V^2, \tag{8}$$

where C_m is the moment coefficient; and L_m is the under-water path length.

3   Basic Equations

Let ($\mathbf{i}$, $\mathbf{j}$, $\mathbf{k}$) be the unit vectors of the Cartesian coordinate system fixed to the Earth with ($\mathbf{i}$, $\mathbf{j}$) in the horizontal plan and $\mathbf{k}$ in the vertical (positive upward). Time derivative of (2a) gives the acceleration of COM (Chu et al., 2006a, b),

$$\frac{d\mathbf{u}}{dt} = \frac{dV}{dt}\mathbf{e}_v + V\frac{d\mathbf{e}_v}{dt}. \tag{9}$$

If the translation velocity has an elevation angle γ and an azimuth angle ψ, the unit vector $\mathbf{e}_v$ is represented by

$$\mathbf{e}_v = \cos\gamma\cos\psi\mathbf{i} + \cos\gamma\sin\psi\mathbf{j} + \sin\gamma\mathbf{k}, \tag{10}$$

Substitution of (10) into (9) leads to

$$\frac{d\mathbf{e}_v}{dt} = \frac{d\gamma}{dt}\mathbf{e}_v^\gamma + \frac{d\psi}{dt}\mathbf{e}_v^\psi, \tag{11}$$

where

$$\mathbf{e}_v^\gamma = -\sin\gamma\cos\psi\mathbf{i} - \sin\gamma\sin\psi\mathbf{j} + \cos\gamma\mathbf{k}, \quad \mathbf{e}_v^\psi = -\cos\lambda\sin\psi\mathbf{i} + \cos\lambda\cos\psi\mathbf{j}, \tag{12}$$

$$\mathbf{e}_v^\gamma \perp \mathbf{e}_v, \quad \mathbf{e}_v^\psi \perp \mathbf{e}_v, \quad \mathbf{e}_v^\gamma \perp \mathbf{e}_v^\psi. \tag{13}$$

The momentum equation is given by

$$m\frac{dV}{dt}\mathbf{e}_v + mV(\frac{d\gamma}{dt}\mathbf{e}_v^\gamma + \frac{d\psi}{dt}\mathbf{e}_v^\psi) = (\rho\Pi - m)g\mathbf{k} - f_d\mathbf{e}_v + f_l\mathbf{e}_l. \tag{14}$$

where (m, Π) are the mass and volume of the rigid body; (f_d, f_l) are the drag and lift forces. Let $\boldsymbol{\Omega}^*$ be the body's angular velocity, which is decomposed into two

parts with the one along the unit vector $\mathbf{e}$ (self-spinning or bank) and the other part $\mathbf{\Omega}$ (azimuth and elevation) perpendicular to $\mathbf{e}$,

$$\mathbf{\Omega}^* = \Omega_s \mathbf{e} + \Omega \mathbf{e}_\omega, \qquad \mathbf{e}_\omega \cdot \mathbf{e} = 0, \tag{15}$$

where $\mathbf{e}_\omega$ is the unit vector of $\mathbf{\Omega}$ (perpendicular to $\mathbf{e}$),

$$\mathbf{\Omega} = \Omega \mathbf{e}_\omega \qquad \Omega = |\mathbf{\Omega}|. \tag{16}$$

For axially symmetric body, $\mathbf{J}$ is a diagonal matrix

$$\mathbf{J} = \begin{bmatrix} J_1 & 0 & 0 \\ 0 & J_2 & 0 \\ 0 & 0 & J_3 \end{bmatrix}, \tag{17}$$

with J_1, J_2, and J_3 the moments of inertia. The moment of momentum equation for small self-spinning velocity is given by (Chu and Fan, 2007)

$$\mathbf{J} \cdot \frac{d\mathbf{\Omega}}{dt} \approx \sigma \rho \Pi g \mathbf{e} \times \mathbf{k} + \sigma \left(f_d \mathbf{e} \times \mathbf{e}_d + f_l \mathbf{e} \times \mathbf{e}_l \right) + \mathbf{M}_t + \mathbf{M}_{ae}. \tag{18}$$

where $\mathbf{M}_{az}$ is the torque due to the azimuth and elevation rotation,

$$\mathbf{M}_{ae} = \frac{1}{2} \mathbf{e}_\omega \int_{-L/2}^{L/2} C_r \rho D (V_r - x\Omega)^2 \, x\,dx = -\frac{1}{12} C_r \rho D L^3 V_r \Omega \mathbf{e}_\omega, \qquad \text{for } \frac{\Omega L}{2} \le V_r$$

$$\mathbf{M}_{ae} = \mathbf{e}_\omega \left[\int_{-\frac{L}{2}}^{\frac{V_r}{\Omega}} \frac{1}{2} C_r \rho D (V_r - x\Omega)^2 \, x\,dx - \int_{\frac{V_r}{\Omega}}^{\frac{L}{2}} \frac{1}{2} C_r \rho D (V_r - x\Omega)^2 \, x\,dx \right]$$

$$= -\frac{1}{2} C_r \rho D L^2 \left[V_r^2 \left(\frac{1}{4} - \left(\frac{V_r}{\Omega L} \right)^2 \right) + \frac{4}{3} V_r \Omega L \left(\frac{V_r}{\Omega L} \right)^3 + \frac{1}{2} \Omega^2 L^2 \left(\frac{1}{16} - \left(\frac{V_r}{\Omega L} \right)^4 \right) \right] \mathbf{e}_\omega$$

$$\text{for } \frac{\Omega L}{2} > V_r.$$

4. Hydrodynamic Coefficients

Prediction of the rigid-body's orientation and COM location is to integrate the momentum equation (14) and moment of momentum equation (18) with known coefficients: C_d, C_l, and C_m. Inner products between equation (14) and the unit vectors ($\mathbf{e}_v$, $\mathbf{e}_v^\gamma$, $\mathbf{e}_v^\psi$) give (Chu et al., 2008)

$$C_d = \frac{(\rho \Pi - m) g \mathbf{k} \cdot \mathbf{e}_v - m \dfrac{dV}{dt}}{\dfrac{1}{2} \rho A_w |V| V}, \tag{19}$$

$$C_l = \frac{mV\left(\mathbf{e}_v^{\gamma}d\gamma/dt + \mathbf{e}_v^{\psi}d\psi/dt\right)\bullet\mathbf{e}_l - \left(\rho\Pi - m\right)g\mathbf{k}\bullet\mathbf{e}_l}{\frac{1}{2}\rho A_w|V|V}. \qquad (20)$$

Inner product of (18) by the vector $\mathbf{e}_r$ leads to

$$C_m = \frac{\mathbf{J}\bullet\dfrac{d\mathbf{\Omega}}{dt}\bullet\mathbf{e}_r - \sigma\rho\Pi g\left(\mathbf{e}\times\mathbf{k}\right)\bullet\mathbf{e}_r}{\frac{1}{2}\rho A_w L_w V^2} - \frac{\sigma}{L_w}\left(C_d\left(\mathbf{e}\times\mathbf{e}_d\right)\bullet\mathbf{e}_r + C_l\left(\mathbf{e}\times\mathbf{e}_l\right)\bullet\mathbf{e}_r\right), \quad (21)$$

where

$$\mathbf{e}_r = \mathbf{e}_\omega\times\mathbf{e}, \quad V_r = \mathbf{V}\bullet\mathbf{e}_r. \qquad (22)$$

The formulas (19)-(21) provide the basis for the experimental determination of (C_d, C_l, C_m) since each item in the right-hands of (19)-(21) can be measured by experiment.

5 Bomb Drop Experiment

Models of Mk-84 bombs with and without tail section are taken as examples to illustrate the methodology for determination of the bulk drag/lift coefficients, and in turn the prediction of location and orientation of a fast-moving rigid-body through the water column. The primary objective is to determine the Mk84 trajectory through the very shallow water zone to provide an estimate of the maximum bomb-to-target standoff and required fuse delay time for optimum target lethality. Using the Hopkins scaling laws, 1/12-scale Mk84 bomb models were designed and constructed in SRI that matched the overall casing shape and mass inertial properties of the full-scale Mk84 prototype. The models were accelerated to velocities of up to about 454 m s^{-1} using a gas gun. The gun was positioned over a 6 m deep by 9 m diameter pool, located at SRI's Corral Hollow Experiment Site (CHES). Two orthogonal Phantom 7 high-speed video (HSV) cameras operating at 10,000 fps were used to record the water entry and underwater trajectory. The digital HSV data were used to generate depth versus horizontal trajectory, position-time history, velocity-time history, deceleration-time history, and drag coefficient-time history profiles. Typically, up to three experiments were performed for each model configuration to determine the overall reproducibility (Gefken, 2006).

A gas gun with 0.10 m (4 in.) diameter and 1.52 m (60-in.) long was positioned over a 6.10 m (20-ft) deep by 9.14 m (30-ft) diameter pool located at SRI's Corral Hollow Experiment Site (CHES). At the end of the gas gun there was a massive steel ring to strip the sabot from the scale model. At high velocities there is some deviation from the theoretical calibration curve, which may be attributed to gas

blow by around the sabot or friction. For the maximum gun operating pressure of 2,500 psi, we were able to achieve a nominal water-entry velocity of about 304.80 m/s. A series of 19 experiments was performed with the different 1/12-scale Mk84 bomb models described in subsection 6.2 with nominal water-entry velocities ranging from 119.48 m/s to 308.83 m/s (Table 1).

Table 1. Summary of Mk84 underwater trajectory experimental matrix.

Experiment Number	Model Type		Water-Entry Velocity (m/s)	Water-Entry Impact Angle (^{o})
1	I		131.51	89.2
2	I		296.87	90.0
3	I		295.35	88.8
4	I		302.05	88.5
5	I		226.77	88.0
6	I		219.45	89.0
7	I		119.48	88.2
8	II	Model	impacted sabot	stripper plate
9	II	Model	impacted sabot	stripper plate
10	II		295.04	90.0
11	II		289.96	90.0
12	II	Model	impacted sabot	stripper plate
13	IV		296.26	85.7
14	IV		300.53	90.0
15	IV		300.53	88.7
16	III		304.19	90.0
17	III		298.39	87.0
18	III		291.08	88.1
19	II		296.87	90.0

6 Semi-Empirical Formulas

Upon completion of the drop phase, the video from each camera was converted to digital format. For Mk84 warhead without tail section, vertical and horizontal locations of the two-end points (Fig. 3) versus time were recorded. From these data, the unit vector **e** can be directly determined using (1b). The translation velocity **u** and the angular velocity **Ω** are measured and so as the fluid-to-body relative velocity **V** since it is assumed that the water velocity is much smaller than the bomb velocity [i.e., (2b) holds]. The unit vectors ($\mathbf{e}_v$, $\mathbf{e}_l$) are in turned determined since ($\mathbf{e}_v$, $\mathbf{e}_l$) represent the direction of **V** and its 90° shift. When the

orientation of the bomb is measured, the unit vector $\mathbf{e}$ is known and so as $\mathbf{e}_\omega$ using (22).
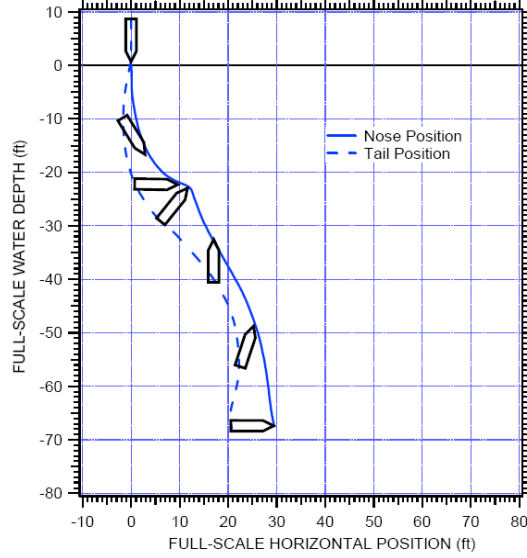

Fig. 3. Trajectory of Mk84 with no tail section and water-entry velocity of 296 m/s (Exp-13) (from Gefken, 2006).

Using the unit vector $\mathbf{e}_v$, we determine the elevation angle γ and the azimuth angle ψ [see (10)] and the two other unit vectors ($\mathbf{e}_v^\gamma, \mathbf{e}_v^\psi$) [see (11)]. Using the unit vectors $\mathbf{e}$ and $\mathbf{e}_\omega$, we determine the unit vector $\mathbf{e}_r$ [see (22)]. With the calculated temporally varying (C_d, C_l, C_m) and (α, Re) data, we obtain the following semi-empirical formulas for calculating the hydrodynamic coefficients,

$$C_d(\text{Re},\alpha) = \begin{cases} 8\sin(2\alpha)\left(\dfrac{\text{Re}_{crit}}{\text{Re}}\right)^2 + 0.02 & \text{if } \sin(2\alpha) \geq 0 \text{ and } \text{Re} \geq \text{Re}_{crit} \\[4mm] 0.34\left|\sin(2\alpha)\right|\left(\dfrac{\text{Re}_{crit}}{\text{Re}}\right) + 0.02 & \text{otherwise} \end{cases} \quad , \quad (33)$$

$$C_l(\text{Re},\alpha) = \begin{cases} 2.5\sin(2\alpha)\min\left[\left(\dfrac{\text{Re}}{\text{Re}_{crit}}\right)^{1.2}, \left(\dfrac{\text{Re}_{crit}}{\text{Re}}\right)^{1.2}\right] & \text{if } \sin(2\alpha) \geq 0 \\[4mm] 0.16\sin(2\alpha) & \text{if } \sin(2\alpha) < 0 \end{cases} \quad , \quad (34)$$

$$\text{Re}_{crit} = 1.5 \times 10^7,$$

$$C_m = A\sin\theta - B\frac{d\alpha}{dt}, \quad A = \begin{cases} 0.06 & \text{if } \theta \leq 180 \\ 0.006 & \text{if } \theta > 180 \end{cases}, \quad B = 0.00065. \quad (35)$$

7. Verification

The semi-empirical formulas of (C_d, C_l, C_m) were verified using the data collected from the experiments. We use the formulas (33)-(35) to compute the hydrodynamic coefficients (C_d, C_l, C_m), and then to predict the location and orientation of Mk-84 bomb in the water column by (14) and (18). Comparison between model predictions and experiments (Fig. 4) shows the validity of feasibility of the semi-empirical formulas (33)-(35).
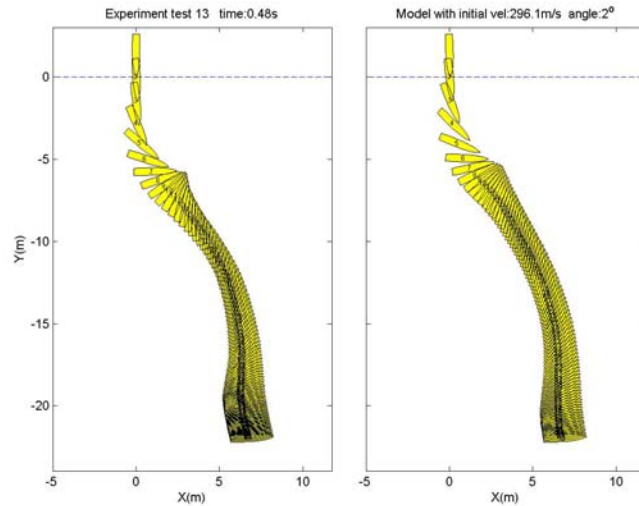

Fig. 4. Comparison between modelled and observed bomb trajectories for the experiment shown in Fig. 3.

8. Conclusions

A new method has been developed to determine the hydrodynamic coefficients (C_d, C_l, C_m) of fast-moving rigid body in the water column. This method contains two parts: (1) establishment of the inverse relationship between (C_d, C_l, C_m) and the rigid-body's trajectory and orientation, and (2) experiments for collecting data of the rigid-body's trajectory and orientation. Using the experimental data, the inverse relationship leads to semi-empirical formulas of (C_d, C_l, C_m) versus Reynolds number and attack angle. This method is much cheaper than the traditional one using the wind tunnel to determine (C_d, C_l, C_m). We also verify these formulas using the experimental data.

Acknowledgments

References

Almquist, J. B., 2006: Demonstration of JABS, personal communication.

Chu, P.C., C.W. Fan, A. D. Evans, and A. Gilles, 2004: Triple coordinate transforms for prediction of falling cylinder through the water column. Journal of Applied Mechanics, 71, 292-298.

Chu, P.C., A. Gilles, and C.W. Fan, 2005a: Experiment of falling cylinder through the water column. Experimental and Thermal Fluid Sciences, 29, 555-568.

Chu, P.C., and C.W. Fan, 2005b: Pseudo-cylinder parameterization for mine impact burial prediction. Journal of Fluids Engineering, 127, 1515-152.

Chu, P.C., and C.W. Fan, 2006a: Prediction of falling cylinder through air-water-sediment columns. Journal of Applied Fluid Mechanics, 73, 300-314.

Chu, P.C., and G. Ray, 2006b: Prediction of high speed rigid body maneuvering in air-water-sediment columns. Advances in Fluid Mechanics, 6, 123-132.

Chu, P.C., and C.W. Fan, 2007: Mine impact burial model (IMPACT35) verification and improvement using sediment bearing factor method. IEEE Journal of Oceanic Engineering, 32 (1), 34-48.

Chu, P.C., C.W. Fan, and P. Gefken, 2008: Dynamical-experimental determination of bulk drag/lift coefficients for high speed rigid body in water column. Advances in Fluid Mechanics, 7, 163-172.

Chu, P.C., C.W. Fan, and P. R. Gefken, 2009: Semi-empirical determination of drag/lift/torque coefficients of high speed rigid body in water column. Journal of Applied Mechanics, in press.

Gefken, P., 2006: Evaluation of precision-guided bomb trajectory through water using scaled-model experiments. SRI Final Technical Report-PYU-16600, Menlo Park, California, USA, 1-80.